TopEros model: Integrating hydrology and multi-process erosion modelling at catchment scale

Emmanuel Okiria[1, *], Keigo Noda[2], Shin-ichi Nishimura[3] and Yukimitsu Kobayashi[4]

[1] Centre for Climate Change Adaptation, National Institute for Environmental Studies, Tsukuba, Japan
[2] Graduate School of Agricultural and Life Sciences, The University of Tokyo, Tokyo, Japan
[3] Faculty of Applied Biological Sciences, Gifu University, Gifu, Japan
[4] NTC-International Co., Ltd., Tokyo, Japan
[*] Author to whom any correspondence should be addressed

E-mail: okiria.emmanuel@nies.go.jp

Keywords: TopEros; hydro-erosion; sheet erosion, gulley erosion, raindrop detachment, sub-grid zoning

Abstract. Hydro-erosion is a primary driver of soil degradation worldwide, yet accurate catchment-scale prediction remains challenging because sheet, gully, and raindrop-impact detachment processes operate simultaneously at sub-grid scales. We introduce TopEros, a novel hydro-erosion model that integrates the hydrological framework of TOPMODEL with three distinct erosion modules: sheet erosion, gulley erosion, and raindrop-impact detachment. TopEros employs a sub-grid zoning strategy in which each grid cell is partitioned into diffuse-flow (sheet erosion) and concentrated-flow (gulley erosion) domains using threshold values of two topographic indices: the topographic index (TI) and the contributing-area-slope index ($a_i tan\beta$). Applied to the Namatala River catchment in eastern Uganda and calibrated with TI = 15 and $a_i tan\beta$ = 35, TopEros successfully identified sheet-dominated and gully-prone areas. Simulated specific sediment yields ranged from 95 to 155 Mg ha^{-1} yr^{-1}—classified as "high" to "very high"—with gully zones contributing disproportionately large erosion volumes. These results demonstrate the importance of capturing intra-cell heterogeneity: conventional catchment-average approaches can obscure critical erosion hotspots. By explicitly representing multiple soil detachment and transport mechanisms within a unified, process-based framework, TopEros enhances the realism of catchment-scale erosion estimates and supports the precise targeting of soil and water conservation measures.

1. Introduction

Soil erosion by water is a pervasive hydrological phenomenon and remains a dominant driver of soil degradation globally (Gruver, 2013). The accelerated loss of fertile topsoil lowers agricultural productivity and heightens reservoir siltation and degradation of water quality (Labrière et al., 2015). Hydro-erosion involves several mechanisms: detachment by diffuse flow (sheet and inter-rill erosion), detachment by concentrated flow (rill and gulley erosion) and detachment of particles by raindrop impact. Notably, although gullies typically occupy a limited portion of the landscape, they can dominate sediment export from a catchment: often contributing from 10 to 95% of total sediment yield (Nkonge et al., 2023; Poesen et al., 2003). Therefore, their representation is crucial for understanding sediment dynamics and planning effective conservation measures.

Numerous hydro-erosion models have been developed and applied, ranging from empirical erosion models—such as USLE (Wischmeier & Smith, 1978) and its derivatives (RUSLE (Renard et al., 1994) and MUSLE (Williams, 1982), as implemented in SWAT (Neitsch et al., 2011)—to more physically based erosion models in ANSWERS (Beasley et al., 1980), SHESHED (Wicks & Bathurst, 1996) and SHETRAN (Ewen et al., 2000). However, capturing the complexity of erosion processes at catchment scale remains challenging (Cerdà et al., 2013). Empirical models—like USLE, RUSLE and MUSLE—were developed on simple idealised plots in temperate climates in the conterminous United States, with diffuse flow, and are unable to account for channelised flow processes that are experienced at catchment scale (Labrière et al., 2015). In particular, the 1-D USLE slope-length factor (LS) and its variants cannot resolve 3-D surface complexity or predict gulley initiation and growth (Foster, 1982) as cited in Wang et al., (2012). Yet in many cases, these models are extended to the entire catchment without modification or explicit treatment of their limitations (Gwapedza et al., 2018; Sadeghi et al., 2014; Sadeghi & Mizuyama, 2007; Thakuriah, 2023).

To address the shortcomings of the 1-D LS factor in complex 3-D terrains, Moore et al., (1992) and Desmet & Govers, (1996) proposed a physically meaningful slope-length factor (LS_p), explicitly catering for the complex nature of the catchment terrain. Despite this, USLE-type models remain confined to predicting erosion due to diffuse flow (sheet erosion). Some advanced schemes have attempted to address this shortcoming. For example, SHETRAN calculates grid-scale soil erosion along the hillslope—sheet erosion—and the main channel network—gulley erosion—separately. However, beyond the main channel, along the hillslope itself, concentrated flow can occur, leading to gulley type erosion within the gulley features. In other words, the hillslope in a complex catchment may experience both sheet and gulley erosion at certain locations. Wang et al., (2010) tackled this by calculating both sheet erosion and gulley erosion within a grid-scale, with the assumption that each grid cell experiences both types of erosion.

We, however, find some shortcomings in their framework. We perceive that not all grid-cells along a hillslope experience concentrated flow.

Cognisant of this, we proposed an alternative concept of the erosion process at catchment scale. Firstly, all cells experience water erosion due to detachment by rain drop impact and by diffuse surface runoff. Secondly, in addition to detachment by diffuse runoff and rain drop impact, some cells also experience gulley erosion (detachment by channelised flow).

Two challenges then emerge: The first being determining which cells along the hillslope experience concentrated flow. TopEros solves this by identifying the threshold values of a pair of topographic indices —the Topographic Index (TI) (Beven & Kirkby, 1979), which describes the state of saturation of a soil and the $a_i tan\beta$ index (Moore et al., 1988), which describes the erosive power of surface runoff—at which there is a transition from sheet to gulley erosion. This approach allows the selective application of MUSLE in non-gully domains and gully models where channelised flow dominates. The second challenge is estimating the channel width within each cell. Since the study area consists of river widths that are smaller than the resolutions of the finest freely available DEM datasets—12.5 m (JAXA/METI, 2022)—it is impossible to resolve the stream dimensions by these data. Moreover, like reported by Wang et al., (2010, 2012), river widths change as rivers flow from upstream to downstream, making the representation of a river section as a grid-cell a tedious process: each grid cell would have to be of a different size. For these reasons, TopEros adopted the concept of "assumed channel widths". While Wang et al., (2010) reported a power relationship between channel width and upstream contributing area, Poesen et al., (2003) adopted a relationship between peak discharge and the assumed channel width. Given that upstream contributing area is constant for every cell in a catchment, and for simplicity, we adopted the relationship proposed by Wang et al., (2010) (Equation 13).

To our knowledge, this is the first framework that: (i) systematically identifies hillslope cells with gully features using complementary topographic thresholds, and (ii) applies domain-specific erosion models within a single grid-based catchment scheme. We name this approach TopEros. We test TopEros in the Namatala River catchment, eastern Uganda, and evaluate its ability to capture both sheet and gully erosion dynamics across spatial scales. Finally, we discuss the potential of TopEros as a decision-support tool for catchment management under changing land-use and climate conditions.

2 Materials and Methods

2.1 The study area

The Namatala River catchment, originating from Mt. Elgon in eastern Uganda, is majorly a rural, and agricultural catchment, with upland crops in the highland areas and rapid paddy field development projects in the lowland areas. The catchment is drained by the Namatala River, a permanent river with a catchment area of 154 km^2 at the river gauging station (Figure 1 and Extended Data Figure 2). The river flows in a westerly direction within the delineated watershed. Further downstream of the gauging station, it flows in a southwestern direction, making confluence with Manafwa River, and draining into the Mpologoma River system, which finally flows into Lake Kyoga.

Based on the definition of large catchments—catchments of a scale at which water resources are managed and monitored (Ferguson et al., 2018)—Namatala River catchment can be classified as a large catchment. However, from the definition of Singh (1995), by its size alone, it is classified as a mid-sized catchment.

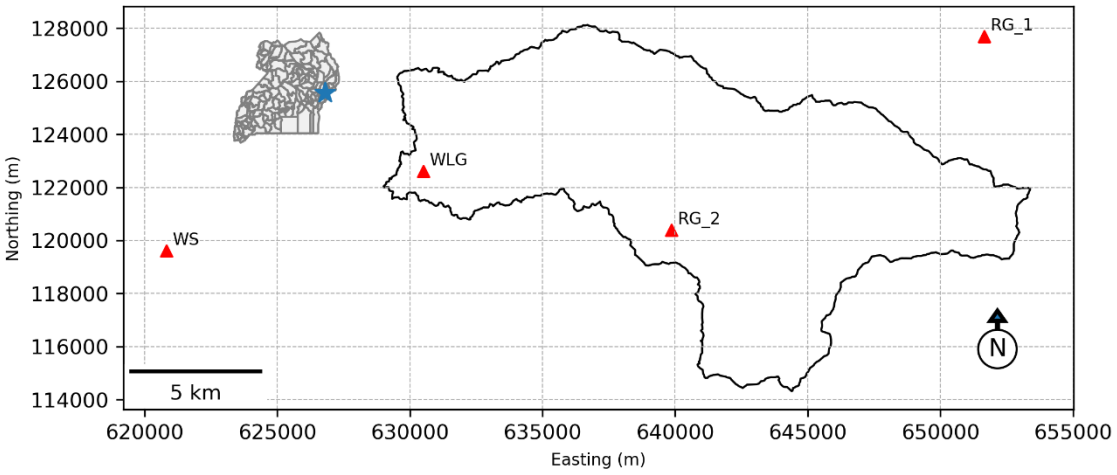

Figure 1: Namatala River catchment. The blue star shows the location of the catchment on the map of Uganda. Note that RG_1 and RG_2 are stations where only rainfall is measured, WS is a weather station—with measurement of 5 meteorological variables—while WLG is the water level gauge along the Mbale-Soroti highway.

2.2 Development of TopEros

The tool for analysis, TopEros (Figure 2), integrates the TOPMODEL concept (Beven & Kirkby, 1979), the FAO56 Penman-Monteith model of reference evapotranspiration (Allen et al., 1998) and three erosion models—MUSLE (Williams, 1982), to predict water erosion by non-concentrated surface runoff; a model to estimate soil detachment by raindrop impact (Foster et al., 1982) and a model to measure soil loss by concentrated flow (Foster et al., 1977)—making it an integration of 5 models. The mathematical formulation of the model was written in Python 3. Various data types, ranging from scalars to 4-D NumPy arrays were adopted. The primary constraint to running the model at fine spatio-temporal resolutions was computing power.

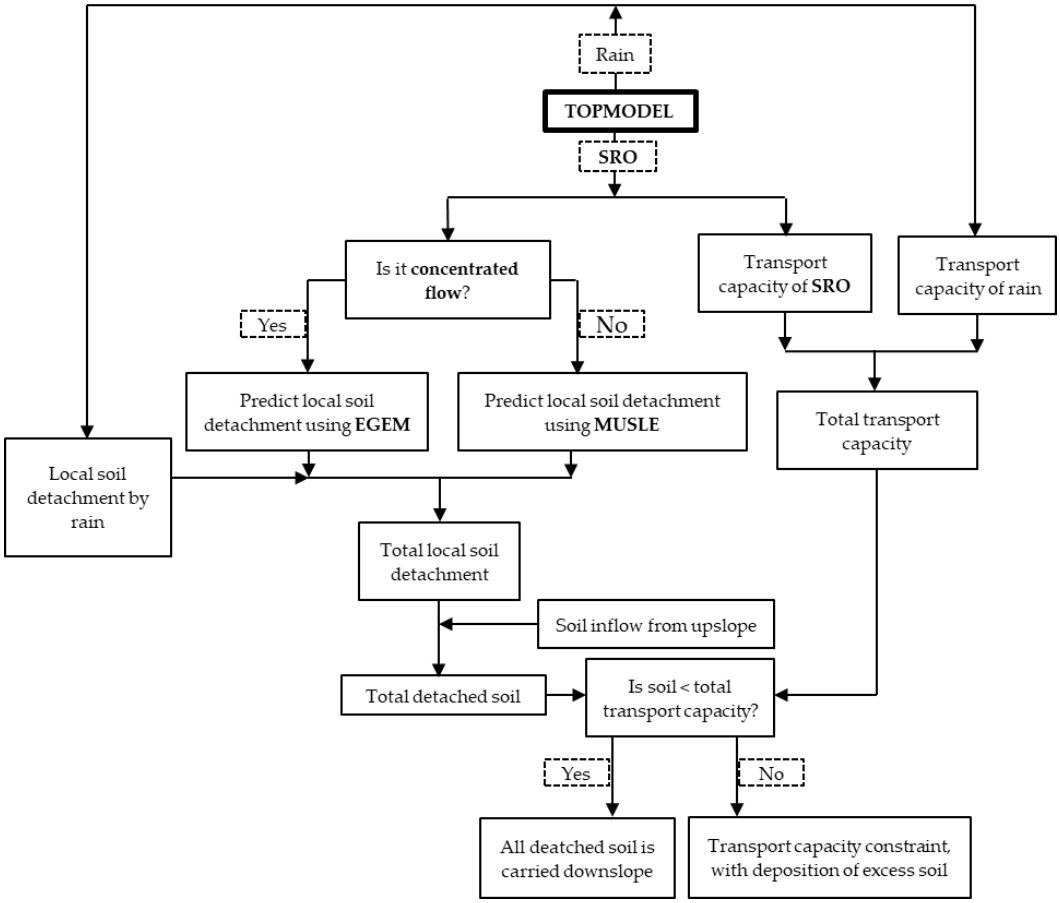

Figure 2: Schematic of the TopEros concept. Note that SRO refers to the surface runoff predicted by the hydrological model; and that EGEM represents the erosion model due to concentrated flow.

2.2.1 Hydrologic Model Component

TOPMODEL is a TOPography-based hydrological model that was put forward by Beven & Kirkby, (1979). It adopts the Topographic Index (TI), an index of hydrological similarity, i.e., cells with the same TI are assumed to have the same hydrologic response, reducing the computational need. From the spatial distribution of TI (**Extended Data Figure 3**), TOPMODEL is also able to track the state of saturation of the soil surface (Beven & Kirkby, 1979; Quinn et al., 1995).

$$TI = \ln\frac{a_i}{\tan\beta_i} \qquad \textbf{Equation 1}$$

Where a_i is the upstream contributing area per unit contour length (Quinn et al., 1995). Speight (1980) defined it as the specific catchment area. Further, Pradhan et al. (2008) defined the "unit contour length" as it pertains to a DEM as the width of a pixel. The term $\tan\beta_i$ is the local slope and *i* is the grid number under evaluation.

TOPMODEL boasts of pros like being spatially distributed; flexible and easily integrated with geographic information systems, allowing for the use of freely available gridded data. Its calibration involves the determination of parameter values like the exponential decay parameter (m); downslope transmissivity (T_e) and the delay time (t_d). The objective functions that were used to test for the model performance were the Nash-Sutcliffe Efficiency (NSE), RMSE-observations standard deviation ratio (RSR) and probability bias (PBIAS) (Foglia et al., 2009; Moriasi et al., 2007). Okiria et al. (2022) have identified the parameter

values for Atari River catchment in eastern Uganda (Extended Data Figure 2). Their study also found that TOPMODEL ably reproduced the hydrological response of catchments in the Elgon region in eastern Uganda. For this reason, TOPMODEL was chosen as the hydrological module for TopEros. A detailed description of the computational procedure of this TOPMODEL can be found in (Beven, 2012; Hornberger et al., 2014; Mukae et al., 2017).

2.2.2 The soil erosion component

Like Wang et al., (2012), each grid cell has an assumed channel. However, unlike their model, where each grid cell simultaneously experienced both sheet and gulley erosion, we posited that: a) All grid cells experience both detachment by raindrop and sheet erosion; b) and that additionally, a grid cell whose topographic index exceeds a certain threshold also experiences gulley erosion within its channels. In other words, each cell can experience "sheet erosion + rain drop splash erosion" and cells with gulleys in them have a duality of "sheet+rain drop splash erosion" and "gulley erosion." However, in each cell, after the erosion process, the eroded soil is carried into the assumed channel for routing to a downstream cell (Note that in non-gulley cells, this hypothetical channel is just a transporter of material and does not experience gulley erosion).
Assumptions of the erosion module:

- Each cell has an assumed channel, whose width is expressed by Equation 13 (Wang et al., 2010).
- Grid cells whose topographic indices exceed a certain threshold, have zones of concentrated flow and exhibit a duality of "sheet+raindrop splash erosion" and "gulley erosion." i.e., sheet erosion due to diffuse runoff in the non-channel zone of the cell, rain drop splash erosion when the soil is not saturated and gulley erosion within the channel section of the cell.
- The hypothetical channel in each cell receives runoff and its entrained sediment for routing to a downstream cell.

The sediment yield is formulated as in Equation *2*.

$$SY = D_{se} + D_{cf} + D_{rd} - SD \qquad \textbf{Equation 2}$$

Where *SY* is sediment yield, D_{se} is the soil detachment due to diffuse runoff, D_{cf} is the soil detachment due to concentrated flow, D_{rd} is soil detachment by rain drop impact and *SD* is sediment deposition. All units are units of mass.

Table 1: Classification of soil loss risk (Jiang et al., 2014)

Erosion risk	Threshold ($Mgha^{-1}yr^{-1}$)
Very low	Soil Loss ≤ 2
Low	2≤Soil Loss≥10
Moderate	10≤Soil Loss≥50
High	50≤Soil Loss≥100
Very high	Soil Loss≥100

Detachment by rain drop

Before becoming saturated, a cell is exposed to detachment by rain drop. Wang et al., (2010) and Foster et al., (1982) proposed a formulation to calculate detachment by effective rain drop energy (Equation 3).

$$D_r = 0.0138KCP^2(2.96\,(tan\,\beta)^{0.79} + 0.56) \qquad \textbf{Equation 3}$$

Where D_r is the soil detachment rate due to rain drop ($kgh^{-1}m^{-2}$), and *K*, and *C* are USLE soil erodibility and crop management factors respectively, while *P* is the effective rainfall intensity (mh^{-1}) and β is the degree slope of the cell.

Sheet erosion detachment

Detachment due to sheet erosion was estimated using MUSLE of Williams, (1982). Its erosion energy factors accept a surface runoff volume and peak discharge rate. The runoff volume and the peak runoff rate are calculated by the hydrological model (TOPMODEL). The critical parameters for MUSLE include among others: the physically derived slope length-slope factor (LS_p) —a measure of the erosive force of the runoff—and the soil erodibility factor (K), a measure of the susceptibility of a soil textural class to erosion. After experimentation, van der Knijff et al., (1999) developed a formulation to estimate USLE's C factor (Equation 5). A formulation for K was suggested by Williams (1995). Further, Moore & Burch, (1986) proposed a physically based formulation of the LS_p factor, hinged on the "unit stream power" theory (Equation 7).

$$D_{se} = 11 \cdot 8\left(Qq_p\right)^{0.56} KCLS_pP \qquad \textbf{Equation 4}$$

D_{se} is the sediment yield due to sheet flow (Mg); Q is the runoff volume (m^3); q_p is the peak runoff rate (m^3s^{-1}) and K, C, and P are the standard USLE factors for soil erodibility, cover management and erosion control practice, respectively. LS_p is the physically derived slope-length factor.

$$C = exp^{\left(-\alpha \cdot \frac{NDVI}{\beta - NDVI}\right)} \qquad \textbf{Equation 5}$$

Parameters α and β determine the shape of the NDVI-C curve. van der Knijff et al., (1999) found that α and β of 2 and 1 respectively yielded reasonable results.

$$K = \left(0.2 + 0.3exp^{[-0.0256SAN(1-\frac{SIL}{100}]}\right)\left(\frac{SIL}{CLA + SIL}\right)^{0.3}\left(1 - \frac{0.25C}{C + exp^{(3.72-2.95C)}}\right)\left(1 \cdot 0 - \frac{0.7SN1}{SN1 + exp^{(-5.51+22 \cdot 9SN1)}}\right) \qquad \textbf{Equation 6}$$

SAN, *SIL*, and *CLA*, and *C* are the percentage sand, silt, clay and organic carbon contents of the soil and SN1 = SAN/100. The edaphic parameters were obtained from the Harmonized World Soil Data Base—Version 1.1 (Nachtergaele et al., 2009). K is allowed to vary from 0 to 0.5.

$$LS_p = \left(\frac{a_i}{22 \cdot 3}\right)^m \cdot \left(\frac{sin\,\beta}{0.0896}\right)^n \qquad \textbf{Equation 7}$$

Where a_i is the upstream contributing area per unit width of contour—analogous to upstream contributing area per unit width of cell) —β is the local degree slope and m, and n are constants. Moore & Burch, (1986) adopted m and n as 0.4 and 1.3, respectively. However, Moore & Wilson, (1992) reported that the RUSLE LS and LS_p were best fitted when exponents m and n were 0.6 and 1.3 respectively. They further reported that values from 0.4 to 0.6—for m—and from 1.2 to 1.3—for n—were reasonable in representing a 3-D complex terrain, which we adopted for our analysis.

Soil erosion by concentrated flow

Each cell experiences detachment by rain drop impact and sheet erosion. However, when the grid-cell's topographic indices exceed a given threshold, the cell will be assumed to experience concentrated flow in its channel section. The cell's channel has assumed width dimensions. In Wang et al., (2010), net flow detachment by concentrated flow occurred when; a) the hydraulic shear stress exceeded the critical shear stress of the soil; and b) when the sediment load was at most, equal to the sediment transport capacity of the flow. The flow detachment capacity was further described as "the gross detachment rate, assuming a uniform distribution of flow and soil erosion rates over the computational grid" (Wang et al., 2010). Here, we modified this to assume a uniform distribution of flow and soil erosion rates over the assumed sub-grid channel reach.

Identification of the location of gulley erosion

Since ephemeral gulley location is controlled by micro-topographies (Moore et al., 1988; Thorne et al., 1986), by extension, all gulley locations can be predicted through topography-derived indices. Moore et al., (1988) found that the combined use of the Topographic Index (TI) and the $a_i tan\beta$ index best predicted gulley locations on a 0.075 km^2 catchment.

Calculation of gulley erosion.

$$D_f = D_{ch}(1 - \frac{G}{T_c}) \quad \textbf{Equation 8}$$

D_f is the net detachment by concentrated flow (kgh^{-1}m^{-2}), D_{ch} is the flow detachment capacity/gross detachment rate (kgh^{-1}m^{-2}) and G is sediment load.

$$D_{ch} = wK(1.35\bar{\tau} - \tau_{cr})^{1.05} \quad \textbf{Equation 9}$$

Where w is the channel width (m), K is USLE's soil erodibility factor, $\bar{\tau}$ is the average shear stress for a cross-section (Pa) and τ_{cr} is the critical shear stress (Pa). The basic form of the equation describing D_{ch} was developed by (Foster et al., 1977). A reformulation of Foster *et al.*'s equation was suggested in Wang et al., (2010) (Equation 9).

$$\tau_{cr\,cr} = 3.23 - 5.6S_a - 24 \cdot 4o_r + 0.0009\rho_{d\,d} \quad \textbf{Equation 10}$$

Where S_a is the fraction of sand in the soil, o_r is the fraction of organic matter in the soil and ρ_d is the dry bulk density of the soil (kgm^{-3}). The formulation of τ_{cr} is in Flanagan & Livingston, (1995).

$$\bar{\tau} = \gamma h S_f \quad \textbf{Equation 11}$$

Where γ (kgm^{-2}s^{-2}) is the specific weight of water and S_f is the friction slope. This formulation is in Wang et al., (2010).

$$S_f = n^2u^2 \,/\, \left(R^{4/3}\right) \quad \textbf{Equation 12}$$

Where n is Manning's roughness co-efficient, u (mh^{-1}) is the depth average of channel flow velocity and R is the hydraulic radius of the assumed channel.

$$w_i = \sigma \cdot A_i^{\varepsilon} \quad \textbf{Equation 13}$$

Where w_i (m) is the assumed channel width at grid i of a rectangular cross-section channel, A_i is the upstream contributing area of grid i and σ and ε are constants. In Wang et al., (2010), while ε=0.5, σ was found by entering the known channel width at the catchment outlet into Equation *13*.

Transport capacity of flow

This is a limit on how much sediment can be carried by runoff (See illustration in Figure 2). Sediment is deposited if the sediment load exceeds the capacity of the runoff to carry it. Beasley et al., (1980) proposed Equation 14 as an estimator of the transport limiting capacity under different rates of discharge.

$$T_c = \begin{cases} 146\,tan\,\beta.\,q^{0.5} & \text{for} \quad q \le 0.046(\mathrm{m}^2/\mathrm{min}) \\ 14600\,\tan\beta.\,\mathrm{q}^2 & \text{for} \quad q > 0.046(\mathrm{m}^2/\mathrm{min}) \end{cases} \quad \textbf{Equation 14}$$

T_c is the transport capacity of the flow per unit width of catchment (kg $min^{-1}m^{-1}$); q is the flow rate per unit width of catchment (m^2min^{-1}) (Moore & Wilson, 1992) and tan β is the local slope.

3 Results and Discussion

TopEros explicitly addresses the inability of traditional USLE-type models to simulate gully erosion or gulley erosion models to predict sheet erosion. It achieves this by dividing the catchment into sheet-erosion and gully-erosion zones, through the adoption of thresholds of two topographic indices—TI and $a_i tan\beta$—to each grid cell. In the Namatala catchment, these thresholds were calibrated to 15 and 35 for TI and $a_i tan\beta$ respectively. This "sheet–concentrated flow duality" allows MUSLE to be applied in sheet-erosion zones and a gully erosion sub-model in zones above the thresholds, thus more realistically capturing the dominant erosion mechanisms in each zone.

Section 3.1 will present results of the calibration of the parameters of the hydrological model—TOPMODEL—while section 3.2 will present findings of the soil erosion models and finally in section 3.3, the limitations of TopEros and future directions will be discussed.

3.1 Calibration and validation of TOPMODEL

Table 2 shows the top 16 parameter sets borne from the calibration of TOPMODEL. From this table, equifinality—where many parameter sets have similar predictive performance—is evident. Through validation of the competing parameter sets against 2016 observed discharge, the first-row parameter set of Table 2—underlined—was chosen as the most optimum, albeit marginally. NSE was 0.616 and 0.503 during calibration and validation respectively. These were deemed acceptable as per Moriasi et al. (2007)'s guidelines. When the monthly mean daily stream discharges were considered, the NSE values increased to 0.881 and 0.879 for calibration and validation respectively, meaning that TOPMODEL simulates monthly runoff values remarkably well. Following Moriasi et al. (2007), this was classified as a "very good" model performance. For the daily averages of stream flow, RSR was 0.619 and 0.705 for the 2015 and 2016 simulation respectively. An analysis of monthly mean averages saw the RSR values improve to 0.345 and 0.347 for calibration and validation respectively, earning a performance rating of "very good" as per Moriasi et al. (2007).

Before discussing percent bias (PBIAS), it is worth noting that different authors formulated and interpreted the metric quite differently (Gupta et al., 1999; Moriasi et al., 2007; Sorooshian et al., 1993; Yapo et al., 1996). In this study, we adopted the method where a positive and a negative PBIAS were synonymous with under estimation and over estimation respectively. (Gupta et al., 1999; Moriasi et al., 2007). For the daily stream discharge, PBIAS was -4.576 % and 1.462 % in calibration and validation periods respectively: within |6.038| percentage points of each other. This was interpreted as a tendency towards the overestimation of stream discharge in 2015 and an opposite tendency in 2016: this can be further visualised in Figure 3 and Figure 4. The inconsistent observations of PBIAS during calibration and validation may seem quite baffling at first. However, given that the absolute values of PBIAS were both close to zero and within |6.038| percentage points of each other, this was deemed not to be an issue of concern.

Figure *3* shows observed daily rainfall, observed daily discharge and simulated daily discharge. Generally, the trend of the observed and simulated hydrograph corresponded well. Most notable was the ability of TOPMODEL to capture both small and large peaks, highlighting the robustness of the variable source area (VSA) concept of the model. A glance at the hydrographs in Figure 3 shows some instances of the underprediction of stream discharge. This could be attributed to localised rainfall events that were missed by the rain gauges. Indeed, Sugawara (1979) reported that tropical rainfall was highly localised, requiring multiple spatially distributed rain gauge networks to get a more meaningful representation of catchment rainfall. With the same logic, the overprediction of peaks could be explained. Though the rainfall event on 2015-June-15 was captured by the rain gauge, it could have been a local event, with minimal effect at catchment scale, hence the higher peaks during simulation. This could be a reason for the higher simulated peak runoff compared to the observed peak after this rainfall event. When the shortcomings of GSMaP rainfall products identified by Takido et al. (2016) are clarified, they—GSMaP products—could complement ground observed data, offering finer spatial resolutions (Okiria et al., 2022) and a more realistic representation of catchment rainfall.

Overall, TOPMODEL robustly simulated catchment runoff, providing a strong foundation for the estimation of erosion due to runoff.

Table 2: The best performing parameter sets from the calibration of TOPMODEL in 2015. Notice the equifinality. The objective functions are calculated for daily averages of stream discharge. NSE_v, RSR_v and PBIAS_v are the corresponding NSE, RSR and PBIAS values during model validation in 2016. Note that SRZinitial was set to 0 in 2016 as the simulation commenced at the start of the rain season.

m (mm)	T_e (mm^2h^{-1})	t_d (hmm^{-1})	*SRmax* (mm)	*SRZinitial* (mm)	NSE	RSR	PBIAS (%)	NSE_v	RSR_v	PBIAS_v
30.847	6879	0.014	2.871	0.000	0.616	0.619	-4.576	0.503	0.705	1.462
33.532	7335	0.012	3.485	0.000	0.611	0.624	-6.519	0.503	0.705	-1.109
30.882	6318	0.013	4.241	0.000	0.608	0.626	-8.091	0.500	0.707	1.108
19.172	9575	0.027	0.331	0.000	0.601	0.631	-5.371	0.486	0.717	6.753
21.879	6328	0.020	3.267	0.000	0.600	0.633	-2.513	0.479	0.722	8.378
28.402	7295	0.020	0.681	0.000	0.589	0.641	4.554	0.491	0.713	7.673
20.713	6593	0.025	2.928	0.000	0.583	0.646	11.930	0.446	0.744	19.357
17.975	9069	0.026	3.605	0.000	0.579	0.649	9.893	0.429	0.756	21.818
23.433	1489	0.026	9.426	0.000	0.553	0.668	10.509	0.387	0.783	22.468
30.605	6169	0.011	5.547	0.000	0.545	0.675	-17.212	0.465	0.731	-6.767
28.797	7571	0.015	9.678	0.000	0.541	0.677	16.338	0.434	0.752	22.765
18.436	8702	0.024	1.719	0.000	0.537	0.681	-9.384	0.473	0.726	7.540
47.187	6869	0.008	7.066	0.000	0.520	0.693	5.980	0.500	0.707	-1.375

41.63	6231	0.012	0.120	0.000	0.51	0.69	-	0.426	0.758	-20.933
1					8	4	23.872			
48.83	2800	0.010	6.340	0.000	0.50	0.70	5.916	0.470	0.728	-1.303
8					1	6				
20.73	3611	0.022	2.884	0.000	0.45	0.74	-	0.438	0.749	0.629
3					2	0	16.854			

Table 3: Objective functions for monthly mean daily stream discharge during calibration and validation of TOPMODEL

	Year	NSE	RSR	PBIAS (%)
Calibration	2015	0.881	0.345	-3.268
Validation	2016	0.879	0.347	1.529

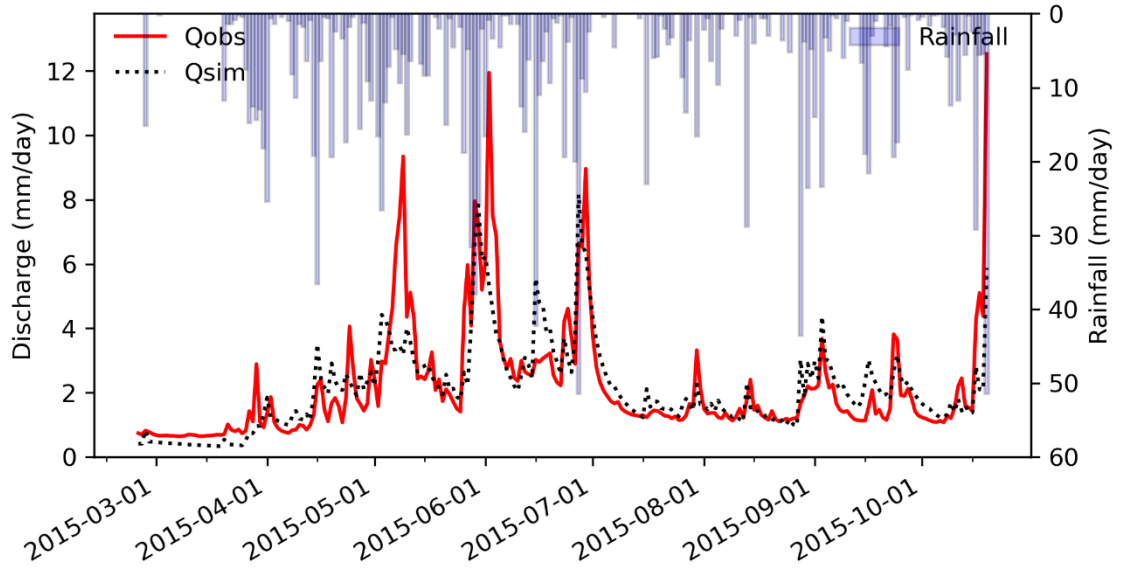

(a)

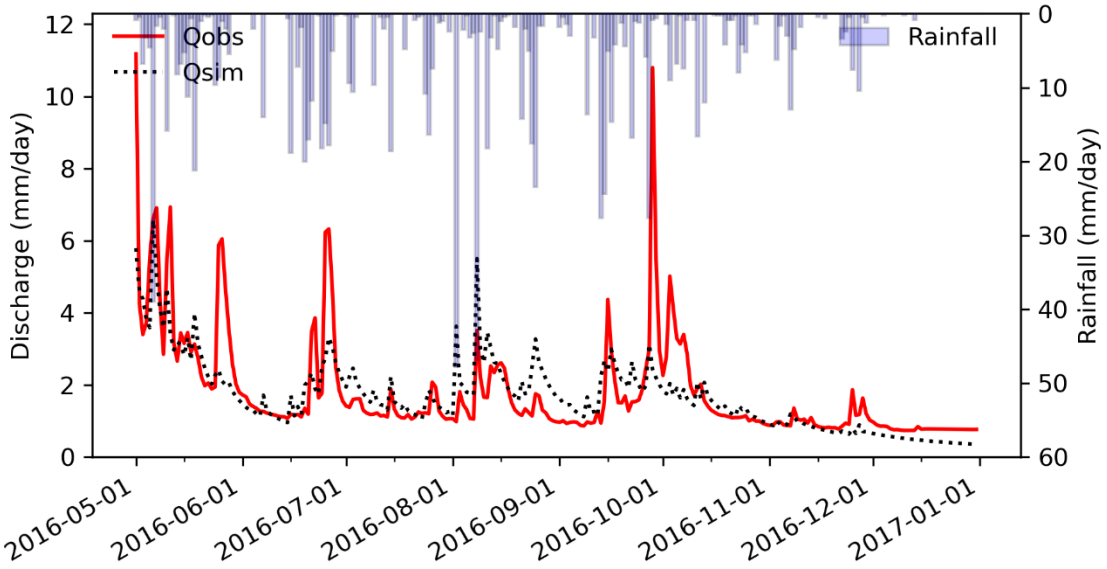

(b)

Figure 3: Observed daily rainfall, observed daily hydrograph and the daily hydrograph simulated by TOPMODEL. Panels (a) and (b) are as predicted in 2015 and 2016 respectively.

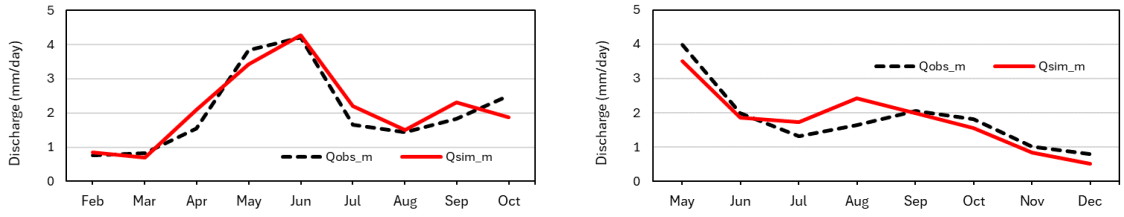

(a) **(b)**

Figure 4: Observed and simulated hydrograph by TOPMODEL. Qobs_m and Qsim_m are observed and simulated monthly mean daily discharges, respectively. Panels (a) and (b) are as predicted in 2015 and 2016, respectively.

3.2 TopEros' Erosion module

With surface runoff generated by TOPMODEL as input, TopEros estimated spatially distributed soil erosion.

3.2.1 MUSLE parameters

The values of the K parameter of MUSLE ranged from 0.127 to 0.204, well within the 0 to 0.5 range defined by Williams (1995)'s Equation 6. Meanwhile, LS_p values varied from 0 to 5.366×10^7. Following the guidelines of Li et al. (2023), for the study period, P=1 was used because there was no evidence of human intervention for soil and water conservation measures within the catchment.

3.2.2 Threshold values of the topographic indices

For Namatala River catchment, the threshold values of TI and $a_i tan\beta$ at which concentrated flow was assumed to start were 15 and 35, respectively. These values predicted the channel features that could be resolved from a 12.5^2 m^2 resolution DEM, aligning with observable stream networks. Moore et al., (1988) reported threshold values of 6.8 and 18 for TI and $a_i tan\beta$ respectively. TI values varying from 6.8 to 9.8 and $a_i tan\beta$ values stretching from 18 to 40 have also been reported (Vandaele et al., 1996). Meanwhile, Daggupati et al., (2013, 2014) reported values of 12 and 30 to 50 for TI and $a_i tan\beta$, respectively. All these values were of the same order of magnitude as those used for TopEros in the Namatala River catchment. This was the first step towards validating the erosion prediction. With the identification of topographic index thresholds, it became possible to predict cells with and without concentrated flow. The caveat is that the threshold values of topographic indices for locating ephemeral gulleys could be site-specific.

3.2.3 Sediment yield at the catchment outlet

Although in situ observations of rainfall for 2015 (February-28 to October-31) and 2016 (May-1 to December-31) were incomplete, they captured most of the bimodal rainfall in the Namatala River catchment—April to May and August to October (Owor, M. et al., 2018). Therefore, annualised units—$Mgyr^{-1}$— provide reasonable approximations of soil erosion. Table 4 and Figure ***5*** summarise sediment yields, deposition and erosion components as simulated by TopEros.

To benchmark the results of TopEros, we also applied MUSLE to the entirety of the catchment. In 2015, TopEros estimated catchment sediment yield (CSY) of 2.387×10^6 Mg yr^{-1}, compared to 2.915×10^6 Mg yr^{-1} from MUSLE. In 2016 the corresponding values were 1.443×10^6 and 1.774×10^6 Mg yr^{-1}, respectively. The tendency of USLE-type models to overpredict sediment yield under high-intensity rainfall has been documented (Benavidez et al., 2018). Desmet & Govers, (1996) and Wischmeier & Smith, (1978) attributed it to non-consideration of sediment deposition process by USLE-type models. However, here, even with the incorporation of sediment deposition, MUSLE still overpredicted sediment yield, exceeding TopEros by ca. 20 % in both years. This could be due to overestimation of the LS_p factor in the channels.

Table 4: Sediment yield, sediment deposition and the gross soil erosion as predicted by TopEros in Namatala River catchment. CSY is the "sediment yield", CSD is the "sediment deposition", CGE_Dof is "catchment gross soil erosion by the sheet erosion process", CGE_Dr is "catchment gross soil erosion by rain drop detachment "and CGE_Df is "catchment gross soil erosion by concentrated flow."

Year	CSY ($Mgyr^{-1}$) $\times 10^6$	CSD ($Mgyr^{-1}$) $\times 10^6$	CGE_Dof ($Mgyr^{-1}$) $\times 10^6$	CGE_Dr ($Mgyr^{-1}$)	CGE_Df ($Mgyr^{-1}$) $\times 10^6$	Model
2015	2.387	4.141	4.438	2.510	2.090	TopEros
2015	2.915	3.697	—	—	—	MUSLE
2016	1.443	3.110	2.714	1.719	1.839	TopEros
2016	1.774	3.697	—	—	—	MUSLE

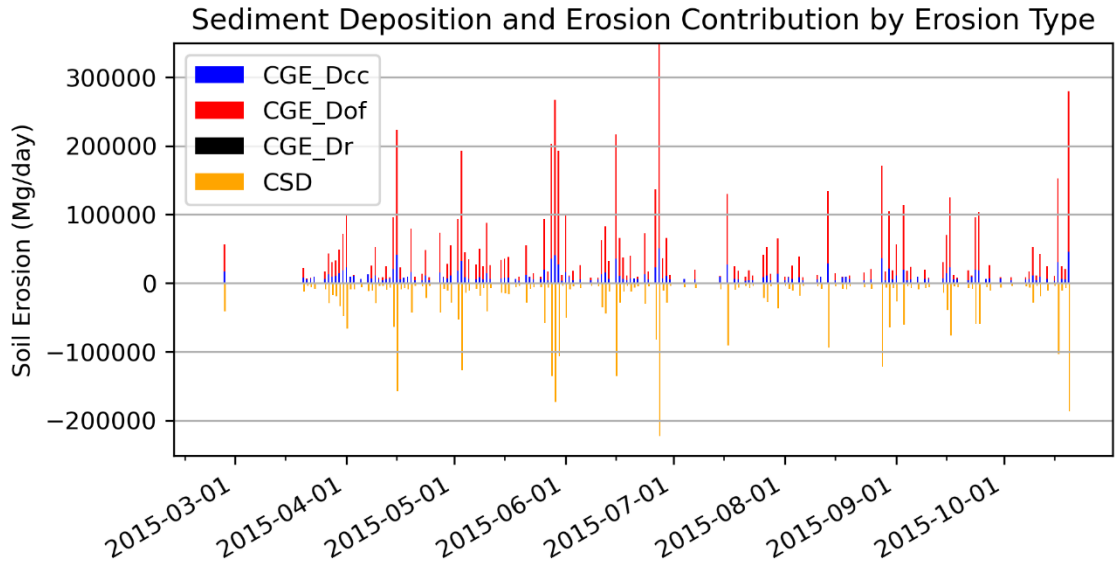

(a)

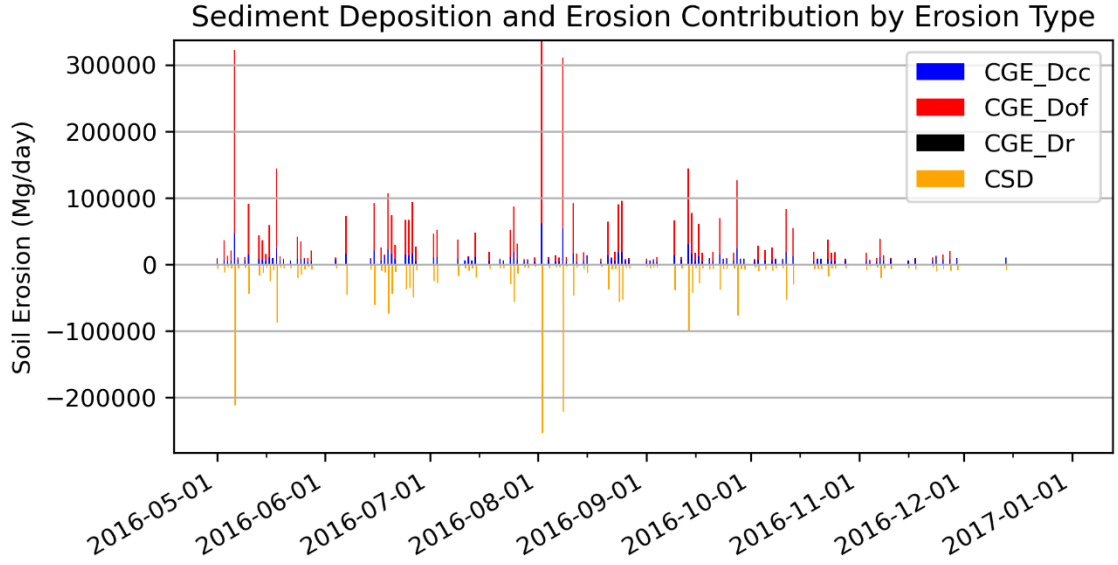

(b)

Figure 5: Daily predicted soil erosion by type and sediment deposition of Namatala River catchment as predicted by TopEros. Panels (a) and (b) are as predicted in 2015 and 2016, respectively.

3.2.4 Partitioning of the erosion process

TopEros enables decomposition of gross erosion into process-specific components. In 2015 sheet (overland) erosion dominated, contributing 68 % (4.438×10^6 Mgyr^{-1}), and in 2016, 60 % (2.714×10^6 Mgyr^{-1}). Given that ca. 90 % of the

catchment area is prone to sheet erosion, these proportions are plausible. Concentrated flow (gulley) detachment accounted for the remaining 32 % (2.090×10^6 Mgyr^{-1}) in 2015 and 40 % (1.839×10^6 Mgyr^{-1}) in 2016, falling within reported gulley-erosion contribution ranges of 10–94 % (Boardman & Poesen, 2006; Poesen et al., 2003). Raindrop detachment was negligible, likely due to rapid surface saturation reducing raindrop impact energy. It is also possible that the climatic and cover management factors in Equation 3 did not consider the effect of throughfall from rain drops that consolidate into larger drops in forested areas with minimal understorey or litter, thereby underestimating erosion by rain drop impact. In their review, Labrière et al., (2015) reported that raindrop amalgamation over large leaves carries more kinetic energy on impact and therefore has greater potential for soil detachment in forested areas without undergrowth.
Yet these partitioned results confirm TopEros's capacity to simulate realistic, process-based erosion magnitudes.

3.2.5 Specific erosion and sediment delivery ratios

To normalise for catchment area and focus on erosion severity, specific soil loss metrics were calculated (Table 5).
Again, we start with benchmarking TopEros against MUSLE. For specific sediment yield (csy), TopEros yielded 155 and 94 Mg ha^{-1}yr^{-1}, versus 190 and 115 Mg ha^{-1}yr^{-1} from MUSLE. Sediment delivery ratio (SDR) further illuminates transport efficiency: TopEros SDRs were 0.366 (in 2015) and 0.317 (in 2016), whereas MUSLE predicted 0.441 and 0.456 in 2015 and 2916 respectively. The empirical relationship of Vanoni (1975) for catchments of this size suggests an SDR of 0.252 (Vanoni 1975, cited in Dhakal et al. 2006; Ouyang and Bartholic 1997). TopEros' closer agreement with Vanoni's benchmark underscores its improved handling of within-catchment erosion and deposition processes.
Secondly, we compared the simulations of TopEros for Namatala River catchment to those from studies on catchments with similar topography and climate. In various Rwandan catchments, Karamage et al., (2016) reported erosion rates ranging from 94 to 678 Mgha^{-1}yr^{-1} using RUSLE: it is worth noting that these values might be higher than the actual sediment yield, because there was no evidence that they accounted for sediment deposition. Similarly, by applying RUSLE to the Manafwa River catchment, a headwater catchment of Mt. Elgon in Uganda, Jiang et al., (2014) reported sediment yields ranging from 67 to 103 Mgha^{-1}yr^{-1}. From their review of observed sediment yields in humid tropical climates globally, Labrière et al., (2015) reported annual erosion rates of 1 to 16 Mgha^{-1}yr^{-1} in humid West African catchments. They also reported values of 0.1, 2 and 5 Mgha^{-1}yr^{-1} in old growth tree, tree crops with and without contact cover respectively. Meanwhile, for humid West African catchments, Morgan, (2005) reported annual erosion rates of 0.03 to 1, 0.1 to 90 and 10 to 750 Mgha^{-1}yr^{-1} in natural, cultivated and bare soil land cover respectively and 1 to 5, 8 to 42 and 5 to 70 Mgha^{-1}yr^{-1} respectively in tropical climates in Ethiopia.

Table 5: Soil Erosion simulation in Namatala River catchment. Note that csy is "catchment specific sediment yield"; csd is "catchment specific sediment deposition, SDR* is "sediment delivery ratio from TopEros" while SDR is "the sediment delivery ratio from the empirical relationship of** Vanoni (1975)**, as cited in** Dhakal et al., (2006); Ouyang & Bartholic, (1997)**.**

Year	csy (Mgha^{-1}yr^{-1})	csd (Mgha^{-1}yr^{-1})	SDR*	SDR**	Model
2015	155	270	0.366	0.252	TopEros
2015	190	241	0.441	0.252	MUSLE
2016	94	202	0.317	0.252	TopEros
2016	115	137	0.456	0.252	MUSLE

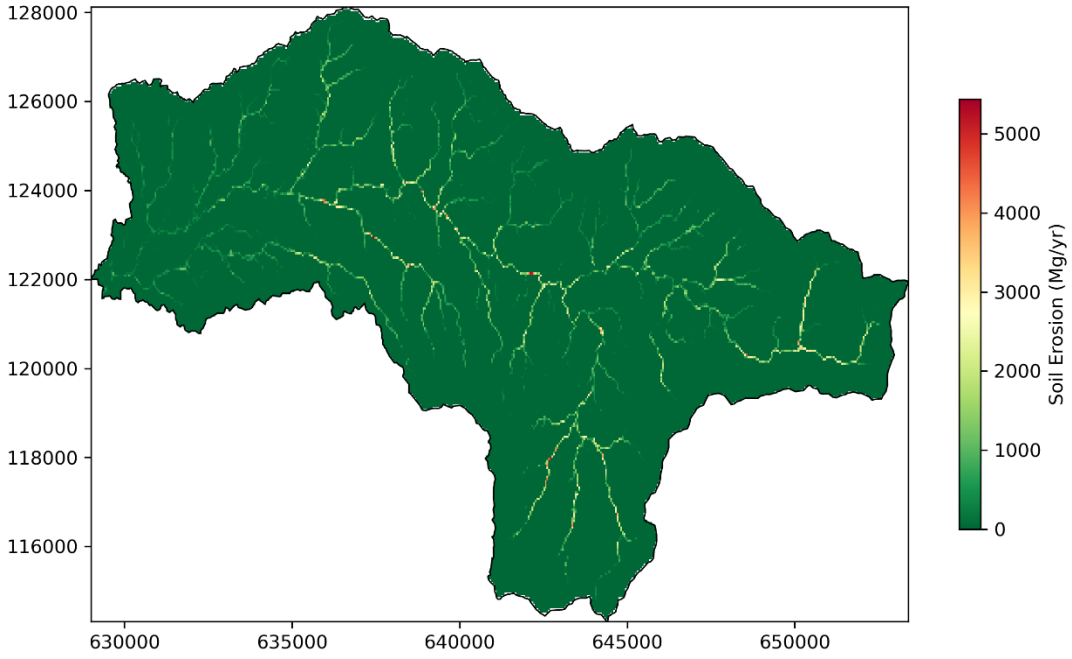
128000
126000
124000
122000
120000
118000
116000
630000
635000
640000
645000
650000
5000
4000
3000
2000
1000
0
Soil Erosion (Mg/yr)

(a)

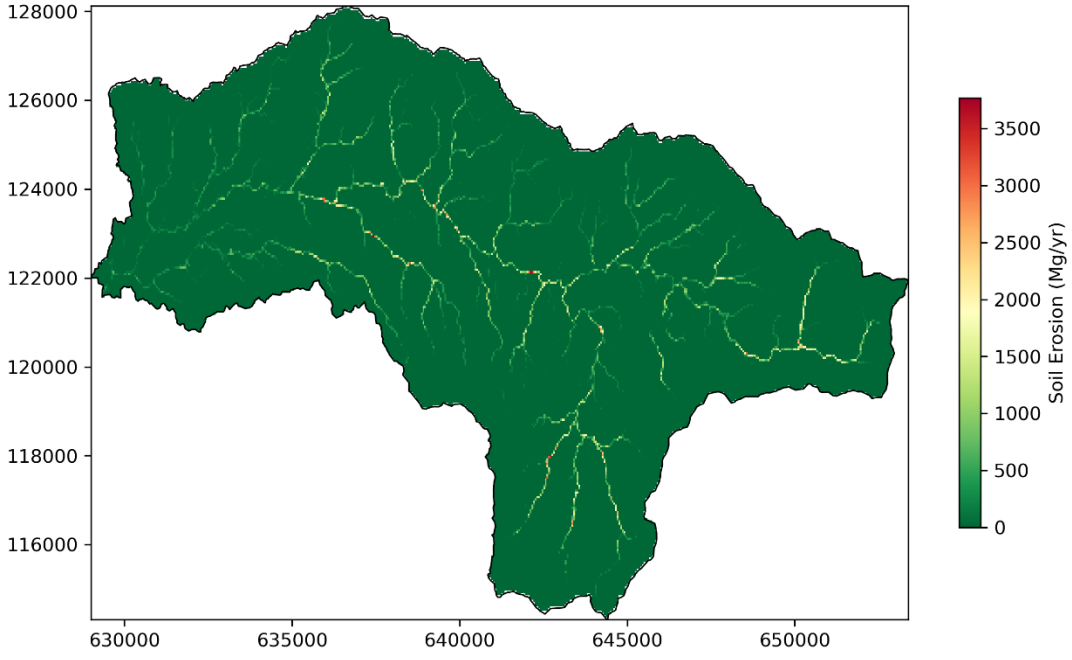
128000
126000
124000
122000
120000
118000
116000
630000
635000
640000
645000
650000
3500
3000
2500
2000
1500
1000
500
0
Soil Erosion (Mg/yr)

(b)

Figure 6: Yearly grid-scale soil erosion of Namatala River catchment as predicted by TopEros. Panels (a) and (b) are as predicted in 2015 and 2016 respectively

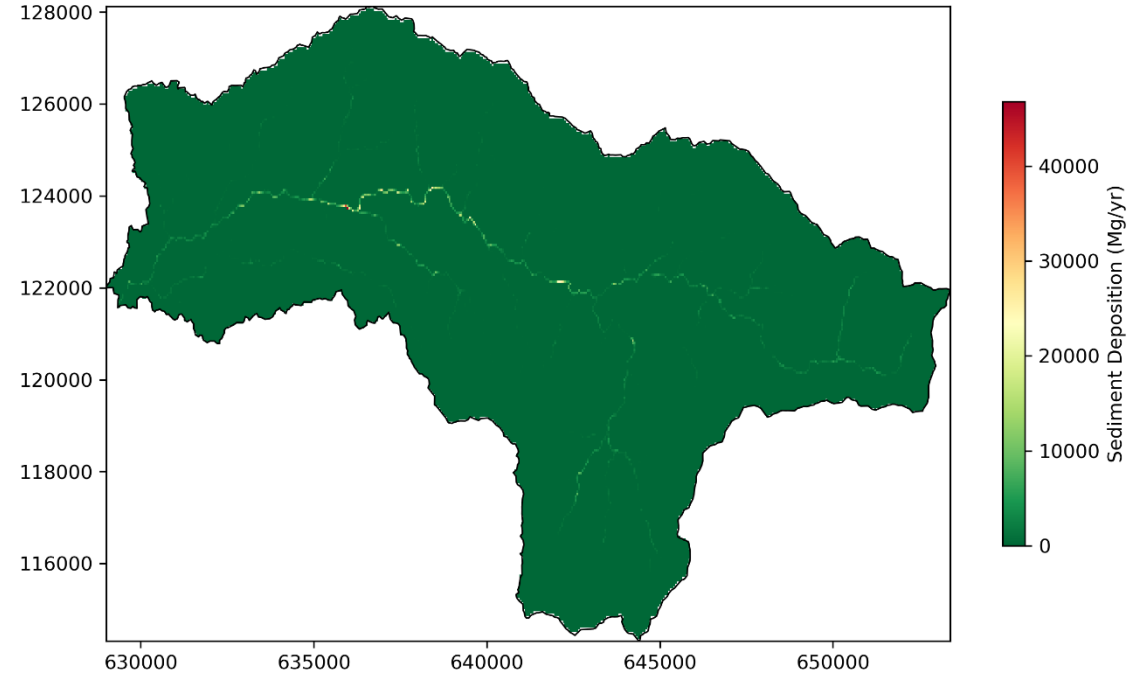

(a)

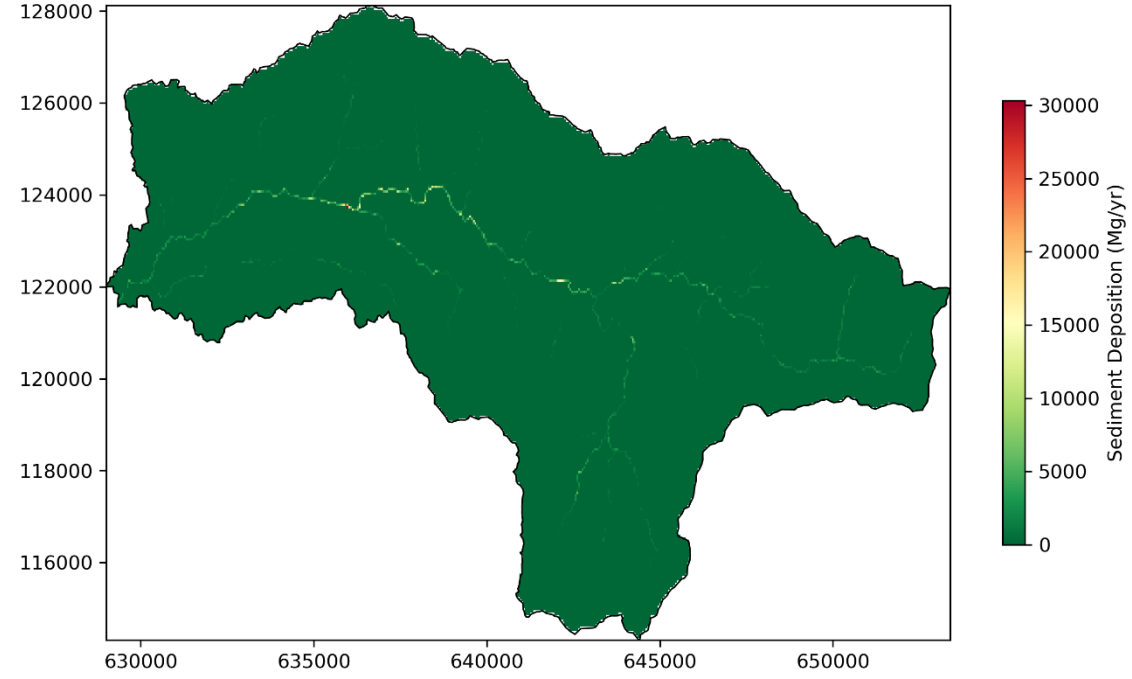

(b)

Figure 7: Sediment deposition in Namatala River catchment as predicted by TopEros. Panels (a) and (b) are as predicted in 2015 and 2016, respectively.

3.2.6 Spatial Patterns and Risk Classification

Figure 6 and Figure 7 illustrate the spatial distribution of annual erosion and deposition. High-erosion hotspots coincided with steep slopes and sparse vegetative cover, while depositional zones clustered in valley bottoms. This spatially explicit output is invaluable for prioritising conservation measures.

Integrating these results into erosion-risk classes (Jiang et al. 2014) yields a catchment-wide classification of "very high" risk in 2015 and "high" in 2016 (Fig. 8). However, gully zones exhibited "very high" risk irrespective of year, whereas non-channel areas largely fall in "low" or "very low" classes. Indeed, gullies enhance sediment connectivity, allowing more sediment to reach the catchment outlet, even when they cover a limited portion of the catchment (Henrique Lima Alencar et al., 2020). This dichotomy highlights the necessity of focused interventions in ephemeral gully networks, supplementing broader sheet-erosion controls.

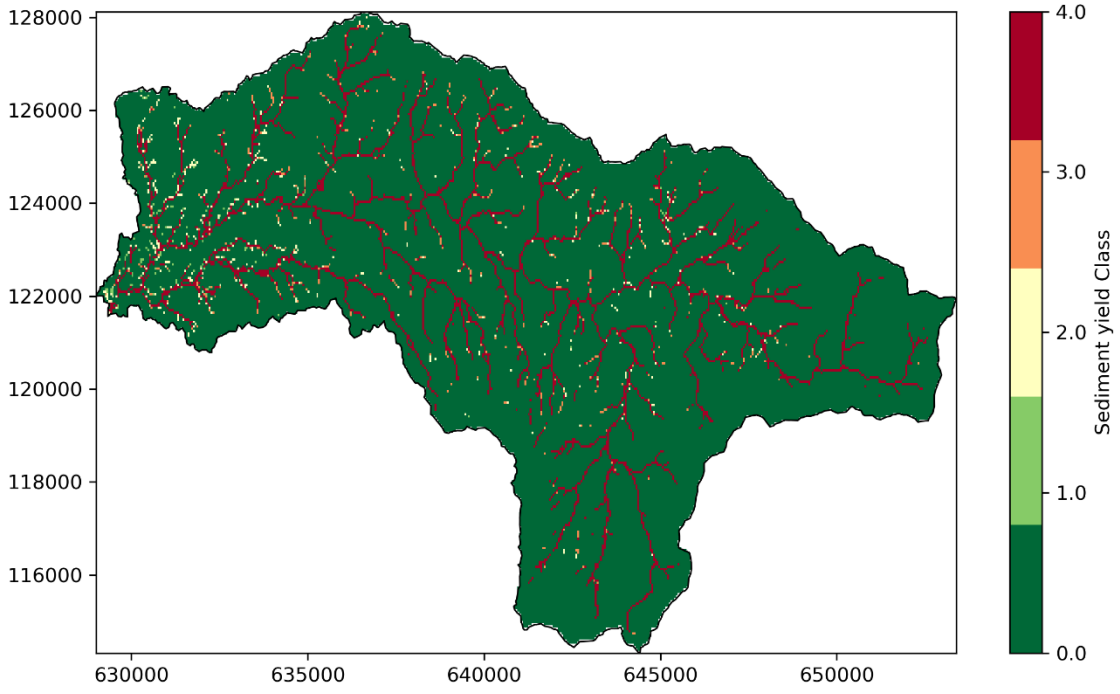

(a)

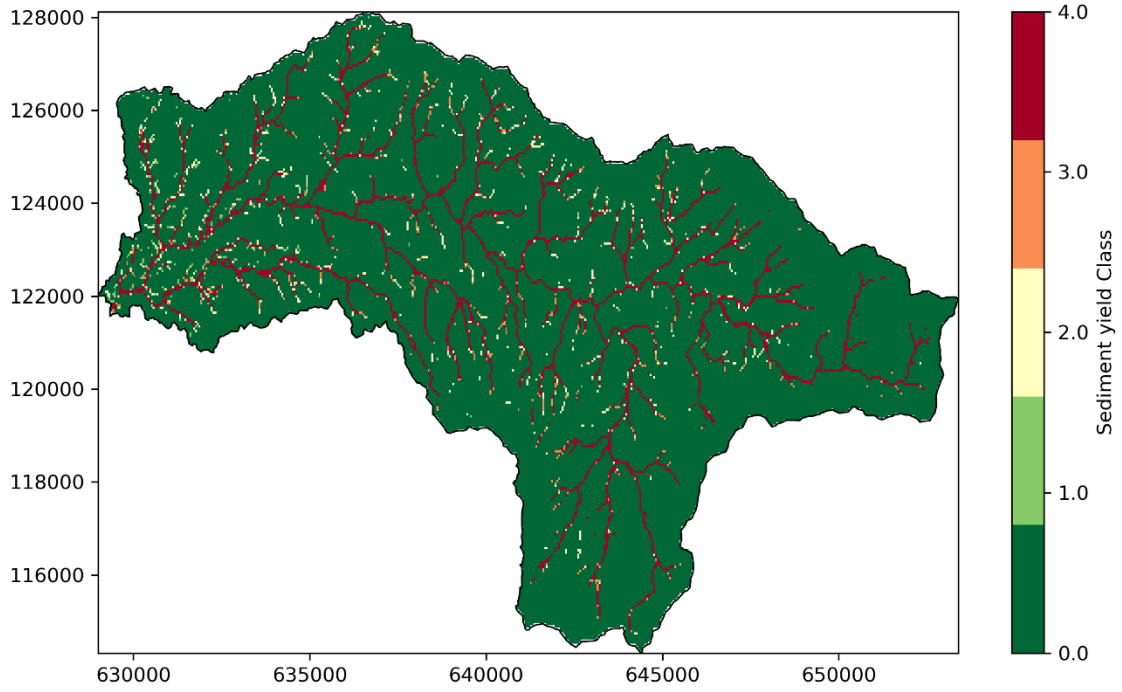

(b)

Figure 8: Erosion risk map of Namatala River catchment. Note that the values 0, 1, 2, 3 and 4 on the colour bar correspond to Jiang et al., (2014) **`s Very Low, Low, Moderate, High and Very High respectively (Table 1). Panels (a) and (b) are as predicted in 2015 and 2016, respectively.**

3.2.7 Model validation and implications

In lieu of direct sediment data, we judged model realism by consistency with known catchment behaviour. Firstly, the locations of large, predicted gulleys align with field-observed channel networks. We also successfully calibrated and validated the runoff model, increasing confidence in the runoff input into the erosion module. Additionally, we found that the SDR predicted by TopEros closely approximated the values predicted by the empirical relationship proposed by Vanoni, (1975). Finally, we compared results from TopEros to those from applying MUSLE in the entire catchment. We went further and compared predictions by TopEros to simulations by RUSLE in catchments in Rwanda and Uganda. A comparison was also made with in situ data in humid tropical climates. Taken together, these increase the confidence in the credibility of TopEros' predictions despite lacking in situ measurements. Future work could target sediment sampling or reservoir survey in Namatala to quantitatively validate the model, but at present the process-based outputs are consistent with both theory and analogous studies.

3.3 Limitations and future directions

While TopEros shows promise, some limitations point to future work. For example, ephemeral gullies are not yet explicitly modelled: their detection could be enhanced by incorporating high resolution optical imagery and or high-resolution DEM analysis. Similarly, the model's robustness should be tested by extending it to other catchments of the Mt. Elgon region and beyond. The model should also consider slope collapse and among other debris flows within a catchment. Finally,

incorporation of a flow routing algorithm into TopEros could; Firstly, improve model performance for larger catchments and secondly, will be a prerequisite for future extension of the model to studies of global soil erosion.

4 Conclusions

We introduced TopEros, a novel process-based hydro-erosion model that couples a TOPMODEL-derived hydrological framework with three dedicated soil-detachment modules: sheet erosion, concentrated-flow (gulley) erosion, and raindrop-impact detachment. By deriving grid cell-specific topographic-index thresholds, TopEros dynamically identifies zones of ephemeral gully formation and applies the most appropriate erosion law in each domain.

Applying TopEros to the Namatala River catchment in eastern Uganda demonstrated its ability to reproduce both annual and sub-grid variability in sediment yield. Compared to the empirically derived MUSLE, TopEros achieved sediment delivery ratios—SDR = 0.366 and 0.317 in 2015 and 2016 respectively—much closer to the Vanoni (1975) benchmark of 0.252, and partitioned gross erosion into realistic process proportions (sheet vs. gulley vs. raindrop detachment). These improvements confirm TopEros's enhanced representation of physical erosion and in-catchment deposition processes.

TopEros thus bridges the gap between plot-scale empirical models and catchment-scale process models by seamlessly integrating distinct detachment mechanisms within a single, spatially distributed framework. This advancement not only refines our conceptualisation of hydro-erosion dynamics at landscape scales but also enables the generation of erosion-risk maps that pinpoint critical hotspots for conservation interventions.

For future work, we recommend:

1. Cross-catchment validation with observed sediment-yield records to quantify TopEros' predictive gains over conventional models.
2. Enhanced gully detection, leveraging high-resolution optical and DEM data, topographic-wetness indices, and targeted field surveys to improve the delineation of ephemeral features.
3. Integration of flow routing modules to extend the model's applicability to larger basins and facilitate eventual upscaling to regional or global soil erosion assessments.

By addressing these limitations, TopEros can become a robust tool for both scientific research and practical catchment management, ultimately supporting more strategic, data-driven soil and water conservation planning.

Code and Data availability

TopEros code and input data can be availed upon request from the authors.

Author contribution

EO and KN developed the concept and designed the experiment, EO wrote the TopEros model code, YK and EO collected and processed the input data, EO conducted the experiment, EO wrote the manuscript with contributions from SN, KN and YK.

Competing Interest

The authors declare that there is no conflict of interest.

Financial support

Funding: This work was supported by JSPS KAKENHI Grant Number 21H05002

References

Allen, R. G., Luis, S. P., RAES, D., & Smith, M. (1998). FAO Irrigation and Drainage Paper No. 56. Crop Evapotranspiration (guidelines for computing crop water requirements). *Irrigation and Drainage*, *300*(56), 300. https://doi.org/10.1016/j.eja.2010.12.001

Beasley, D. B., Huggins, L. F., & Monke, E. J. (1980). ANSWERS: A Model for Watershed Planning. *Transactions, American Society of Agricultural Engineers*, *23*(4), 938–944. https://doi.org/10.13031/2013.34692

Benavidez, R., Jackson, B., Maxwell, D., & Norton, K. (2018). A review of the (Revised) Universal Soil Loss Equation ((R)USLE): With a view to increasing its global applicability and improving soil loss estimates. *Hydrology and Earth System Sciences*, *22*(11), 6059–6086. https://doi.org/10.5194/hess-22-6059-2018

Beven, K. J. (2012). *Rainfall-runoff modelling: the primer* (2nd ed.). Wiley-Blackwell.

Beven, K. J., & Kirkby, M. J. (1979). A physically based, variable contributing area model of basin hydrology. *Hydrological Sciences Journal*, *24*(1), 43–69. https://doi.org/10.1080/02626667909491834

Boardman, J., & Poesen, J. (2006). Soil Erosion in Europe: Major Processes, Causes and Consequences. In J. Boardman & J. Poesen (Eds.), *Soil Erosion in Europe* (pp. 479–487). John Wiley & Sons, Ltd.

Cerdà, A., Brazier, R., Nearing, M., & de Vente, J. (2013). Scales and erosion. In *Catena* (Vol. 102, pp. 1–2). https://doi.org/10.1016/j.catena.2011.09.006

Daggupati, P., Douglas-Mankin, K. R., & Sheshukov, A. Y. (2013). Predicting ephemeral gully location and length using topographic index models. *Transactions of the ASABE*, *56*(4), 1427–1440. https://doi.org/10.13031/trans.56.10087

Daggupati, P., Sheshukov, A. Y., & Douglas-Mankin, K. R. (2014). Evaluating ephemeral gullies with a process-based topographic index model. *Catena*, *113*, 177–186. https://doi.org/10.1016/j.catena.2013.10.005

Desmet, P. J. J., & Govers, G. (1996). A GIS procedure for automatically calculating the USLE LS factor on topographically complex landscape units. *Journal of Soil and Water Conservation*, *51*(5), 427–433.

Dhakal, A., Tsuchiya, S., & Ohsaka, O. (2006). Application of the USLE and Sediment Delivery Models in a Mountainous Catchment. *Journal of Japan Society of Erosion Control Engineering*, *59*(2), 43–48.

Ewen, J., Parkin, G., & O'Connell, P. E. (2000). SHETRAN: Distributed River Basin Flow and Transport Modeling System. *Journal of Hydrologic Engineering*, *5*(3), 250–258.

Ferguson, C. R., Pan, M., & Oki, T. (2018). The Effect of Global Warming on Future Water Availability: CMIP5 Synthesis. *Water Resources Research*, *54*(10), 7791–7819. https://doi.org/10.1029/2018WR022792

Flanagan, D. C., & Livingston, S. J. (1995). *WEPP user summary*. *11*, 141.

Foglia, L., Hill, M. C., Mehl, S. W., & Burlando, P. (2009). Sensitivity analysis, calibration, and testing of a distributed hydrological model using error-based weighting and one objective function. *Water Resources Research*, *45*(W06427). https://doi.org/10.1029/2008WR007255

Foster, G. R. (1982). Modeling the erosion process. In C. T. Haan, H. P. Johnson, & D. L. Brakensiek (Eds.), *Hydrologic modeling of small watersheds* (ASAE Monog, pp. 295–380). ASAE.

Foster, G. R., Lombardi, F., & Moldenhauer, W. C. (1982). Evaluation of rainfall-runoff erosivity factors for individual storms. *Transactions of the ASAE*, *25*(1), 124–129. https://doi.org/10.13031/2013.33490

Foster, Meyer, L. D., & Onstad, C. A. (1977). Erosion Equation Derived From Basic Erosion Principles. *Transactions of the ASAE*, *20*(4), 678–682. https://doi.org/10.13031/2013.35627

Gruver, J. B. (2013). Prediction, Prevention and Remediation of Soil Degradation by Water Erosion. *Nature Education Knowledge*, *4*(12).

Gupta, H. V., Sorooshian, S., & Yapo, P. O. (1999). Status of Automatic Calibration for Hydrologic Models: Comparison with Multilevel Expert Calibration. *Journal of Hydrologic Engineering*, *4*(2), 135–143. https://doi.org/10.1061/(asce)1084-0699(1999)4:2(135)

Gwapedza, D., Hughes, D. A., & Slaughter, A. R. (2018). Spatial scale dependency issues in the application of the Modified Universal Soil Loss Equation (MUSLE). *Hydrological Sciences Journal*, *63*(13–14), 1890–1900. https://doi.org/10.1080/02626667.2018.1546388

Henrique Lima Alencar, P., De Araujo, J. C., & Dos Santos Teixeira, A. (2020). Physically based model for gully simulation: Application to the Brazilian semiarid region. *Hydrology and Earth System Sciences*, *24*(8), 4239–4255. https://doi.org/10.5194/hess-24-4239-2020

Hornberger, G. M., Wiberg, P. L., Raffensperger, J. P., & D'Odorico, P. (2014). *Elements of Physical hydrology* (Second Edi). Johns Hopkins University Press.

JAXA/METI. (2022, July 13). *PALSAR RTC (high resolution)*. JAXA/METI.

Jiang, B., Bamutaze, Y., & Pilesjö, P. (2014). Climate change and land degradation in Africa: A case study in the Mount Elgon region, Uganda. *Geo-Spatial Information Science*, *17*(1), 39–53. https://doi.org/10.1080/10095020.2014.889271

Karamage, F., Zhang, C., Ndayisaba, F., Shao, H., Kayiranga, A., Fang, X., Nahayo, L., Nyesheja, E. M., & Tian, G. (2016). Extent of cropland and related soil erosion risk in Rwanda. *Sustainability (Switzerland)*, *8*(7). https://doi.org/10.3390/su8070609

Labrière, N., Locatelli, B., Laumonier, Y., Freycon, V., & Bernoux, M. (2015). Soil erosion in the humid tropics: A systematic quantitative review. *Agriculture, Ecosystems and Environment*, *203*, 127–139. https://doi.org/10.1016/j.agee.2015.01.027

Li, J., He, H., Zeng, Q., Chen, L., & Sun, R. (2023). A Chinese soil conservation dataset preventing soil water erosion from 1992 to 2019. *Scientific Data*, *10*(1), 1–11. https://doi.org/10.1038/s41597-023-02246-4

Moore, I. D., & Burch, G. J. (1986). Physical basis of the Length-slope Factor in the Universal Soil Loss Equation. *Soil Science Society of America Journal*, *50*(5), 1294–1298.

Moore, I. D., Burch, G. J., & Mackenzie, D. H. (1988). Topographic Effects on the Distribution of Surface Soil Water and the Location of Ephemeral Gullies. *Transactions of the ASAE*, *31*(4), 1098–1107. https://doi.org/10.13031/2013.30829

Moore, I. D., & Wilson, J. P. (1992). Length-slope factors for the revised universal soil loss equation: simplified method of estimation. *Journal of Soil & Water Conservation*, *47*(5), 423–428.

Moore, I. D., Wilson, J. P., & Ciesiolka, C. A. (1992). Soil erosion prediction and GIS: Linking theory and practice. *Proceedings of the International Conference on Application of Geographic Information Systems to Soil Erosion Management*, *November*, 31–48.

Morgan, R. P. C. (2005). *Soil Erosion & Conservation* (3rd ed.). Blackwell Publishing Ltd. chrome-extension://efaidnbmnnnibpcajpcglclefindmkaj/https://svgaos.nl/wp-content/uploads/2017/02/Morgan_2005_Soil_Erosion_and_Conservation.pdf

Moriasi, D. N., Arnold, J. G., Liew, M. W. Van, Bingner, R. L., Harmel, R. D., & Veith, T. L. (2007). Model evaluation guidelines for systematic quantification of accuracy in watershed simulations. *Transactions of the American Society of Agricultural Engineers*, *50*(3), 885–900.

Mukae, K., Miwa, K., & Okazawa, H. (2017). Ecosystem service assessment in agricultural watershed by using TOPMODEL. *AGROFO International Journal*, *2*(3), 27–36. https://doi.org/10.7251/AGRENG1703027F

Nachtergaele, F., Van Velthuizen, H., Verelst, L., Batjes, N., Dijkshoorn, K., Van Engelen, V., Fischer, G., Jones, A., Montanarella, L., Petri, M., Prieler, S., Teixeira, E., Wiberg, D., & Shi, X. (2009). *Harmonized World Soil Database - Version 1.1*.

Neitsch, S. L., Arnold, J. G., Kiniry, J. R., & Williams, J. R. (2011). Soil & Water Assessment Tool Theoretical Documentation Version 2009. *Texas Water Resources Institute*, 1–647. https://doi.org/10.1016/j.scitotenv.2015.11.063

Nkonge, L. K., Gathenya, J. M., Kiptala, J. K., Cheruiyot, C. K., & Petroselli, A. (2023). An Ensemble of Weight of Evidence and Logistic Regression for Gully Erosion Susceptibility Mapping in the Kakia-Esamburmbur Catchment, Kenya. *Water (Switzerland)*, *15*(7). https://doi.org/10.3390/w15071292

Okiria, E., Okazawa, H., Noda, K., Kobayashi, Y., Suzuki, S., & Yamazaki, Y. (2022). A Comparative Evaluation of Lumped and Semi-Distributed Conceptual Hydrological Models: Does Model Complexity Enhance Hydrograph Prediction? *Hydrology*, *9*(5), 89. https://doi.org/10.3390/hydrology9050089

Ouyang, D., & Bartholic, J. (1997). Predicting Sediment Delivery ratio in Saginaw Bay Watershed. *Proceedings of the 22nd National Association of Environmental Professional Conference*, 659–671. www.iwr.msu.edu/rusle/sdr/sag-sdr.htm#:~:text=SDR

Owor, M., Tindimugaya, C., Brown, L., Upton, K., Ó Dochartaigh, B.É. and Bellwood-Howard, I. (2018). *Africa Groundwater Atlas: Hydrogeology of Uganda*. http://earthwise.bgs.ac.uk/index.php/Hydrogeology_of_Uganda

Poesen, J., Nachtergaele, J., Verstraeten, G., & Valentin, C. (2003). Gully erosion and environmental change: importance and research needs. *Catena*, *50*, 91–133. www.elsevier.com/locate/catena

Pradhan, N. R., Ogden, F. L., Tachikawa, Y., & Takara, K. (2008). Scaling of slope, upslope area, and soil water deficit: Implications for transferability and regionalization in topographic index modeling. *Water Resources Research*, *44*(12), 1–12. https://doi.org/10.1029/2007WR006667

Quinn, P. F., Beven, K. J., & Lamb, R. (1995). The ln(a/tanβ) Index: How to Calculate it and How to Use it Within the TOPMODEL Framework. *Hydrological Processes*, *9*, 161–182.

Renard, K. G., Foster, G. R., Yoder, G. C., & McCool, D. K. (1994). RUSLE revisited: Status, questions, answers and the future. *Journal of Soil and Water Conservation*, *49*(3), 213–220.

Sadeghi, S. H. R., Gholami, L., Khaledi Darvishan, A., & Saeidi, P. (2014). A review of the application of the MUSLE worldwide. *Hydrological Sciences Journal*, *59*(2), 365–375. https://doi.org/10.1080/02626667.2013.866239

Sadeghi, S. H. R., & Mizuyama, T. (2007). Applicability of the Modified Universal Soil Loss Equation for prediction of sediment yield in Khanmirza watershed, Iran. *Hydrological Sciences Journal*, *52*(5), 1068–1075. https://doi.org/10.1623/hysj.52.5.1068

Singh, V. P. (1995). Watershed Modeling. In V. P. Singh (Ed.), *Computer Models of Watershed Hydrology* (pp. 1–20). Water Resources Publications.

Sorooshian, S., Duan, Q., & Gupta, V. K. (1993). Calibration of Rainfall-Runoff Models: Application of Global Optimization to the Sacramento Soil Moisture Accounting Model. *Water Resources Research*, *29*(4), 1185–1194. chrome-extension://efaidnbmnnnibpcajpcglclefindmkaj/https://agupubs.onlinelibrary.wiley.com/doi/pdfdirect/10.1029/92WR02617

Speight, J. G. (1980). The role of topography in controlling throughflow generation: a discussion. *Earth Surface Processes*, *5*(2), 187–191. https://doi.org/10.1002/esp.3760050209

Sugawara, M. (1979). Automatic calibration of the tank model / L'étalonnage automatique d'un modèle à cisterne Automatic calibration of the tank model. *Hydrological Sciences Bulletin*, *24*(9). https://doi.org/10.1080/02626667909491876

Takido, K., Saavedra Valeriano, O. C., Ryo, M., Tanuma, K., Ushio, T., & Kubota, T. (2016). Spatiotemporal evaluation of the gauge-adjusted global satellite mapping of precipitation at the basin scale. *Journal of the Meteorological Society of Japan*, *94*(2), 185–195. https://doi.org/10.2151/jmsj.2016-010

Thakuriah, G. (2023). GIS-based revised universal soil loss equation for estimating annual soil erosion: a case of lower Kulsi basin, India. *SN Applied Sciences*, *5*(3). https://doi.org/10.1007/s42452-023-05303-0

Thorne, C. R., Zevenbergen, L. W., Grissinger, L. H., & Murphy, J. B. (1986). Ephemeral gulleys as sources of sediment. *Proc. Fourth Federal Interagency Sed. Conf*, 3.152-3.161.

van der Knijff, J. M., Jones, R. J. A., & Montanarella, L. (1999). Soil erosion risk assessment in Itally. In *European Soil Bureau, European Commission*. https://doi.org/10.3390/f8020052

Vandaele, K., Poesen, J., Marques da Silva, J. R., & Desmet, P. P. J. (1996). Rates and predictability of ephemeral gully erosion in two contrasting environments. *Géomorphologie Relief Processus Environnement*, *2*(2), 83–95. https://doi.org/10.3406/morfo.1996.880

Vanoni, V. A. (1975). Sedimentation Engineering Practice. In *American Society of Civil Engineers, Manuals and Reports on Engineering Practice, No. 54*.

Wang, G., Hapuarachchi, H. A. P., Takeuchi, K., & Ishidaira, H. (2010). Grid-based distribution model for simulating runoff and soil erosion from a large-scale river basin. *Hydrological Processes*, *24*(5), 641–653. https://doi.org/10.1002/hyp.7558

Wang, G., Jiang, H., Xu, Z., Wang, L., & Yue, W. (2012). Evaluating the effect of land use changes on soil erosion and sediment yield using a grid-based distributed modelling approach. *Hydrol. Process*, *26*. https://doi.org/10.1002/hyp.9193

Wicks, J. M., & Bathurst, J. C. (1996). SHESED: A physically based, distributed erosion and sediment yield component for the SHE hydrological modelling system. *Journal of Hydrology*, *175*(1–4), 213–238. https://doi.org/10.1016/S0022-1694(96)80012-6

Williams, J. R. (1982). Testing the Modified Universal Soil Loss Equation. In ER. Burroughs, Jr, JC. Chugg, G. E. Dissmeyer, D. A. Farrell, G. R. Foster, K. A. Gebhardt, G. E. Hart, C. W. Johnson, J. M. Laflen, L. J. Lane, C. J. Lovely, D. K. McCool, L. D. Meyer, W. C. Moldenhauer, E. L. Neff, R. J. Page, K. G. Renard, M. B. Rollins, E. D. Shirley, … JR. Williams (Eds.), *Proceedings of the Workshop on Estimating Erosion and Sediment Yield on Rangelands* (pp. 157–165). U.S. Department of Agriculture, Agricultural Research Service, Agricultural Reviews and manuals ARM - W.

Williams, J. R. (1995). The EPIC Model. In V. P. Singh (Ed.), *Computer Models of Watershed Hydrology* (pp. 909–1000). Water Resources Publications.

Wischmeier, W. H., & Smith, D. D. (1978). *Predicting rainfall erosion losses: a guide to conservation planning* (No. 537). Department of Agriculture, Science and Education Administration.

Yapo, P. O., Gupta, H. V., & Sorooshian, S. (1996). Automatic calibration of conceptual rainfall-runoff models: Sensitivity to calibration data. *Journal of Hydrology*, *181*(1–4), 23–48. https://doi.org/10.1016/0022-1694(95)02918-4

Extended Data

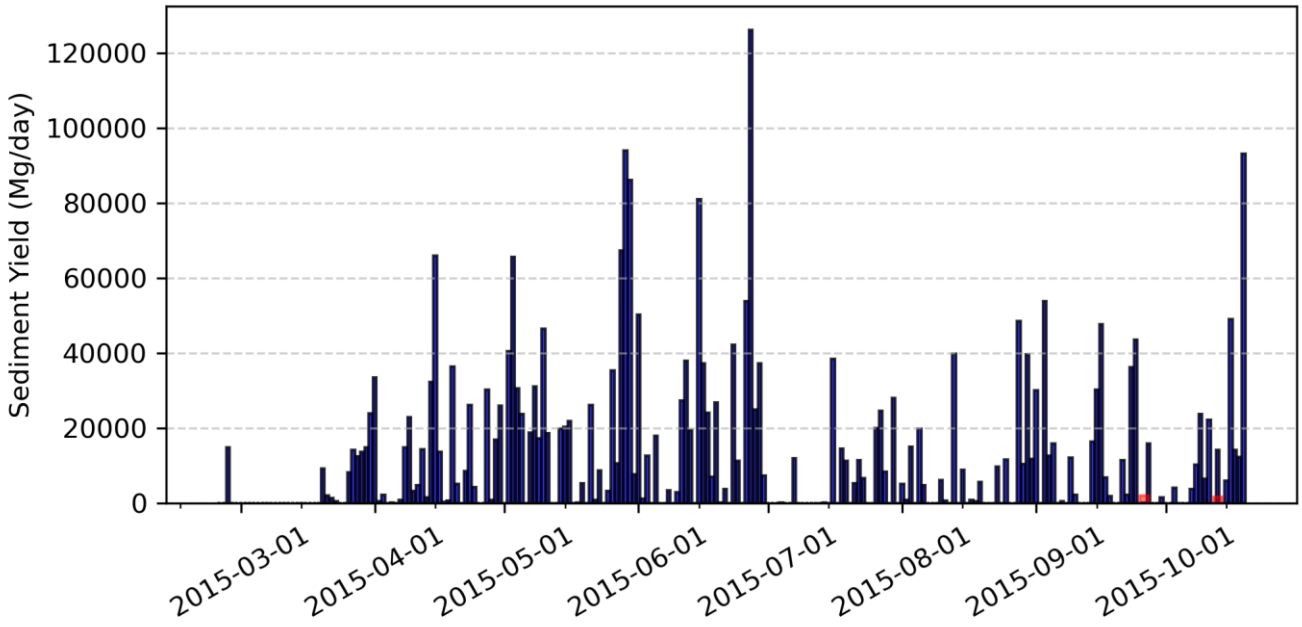

(a)

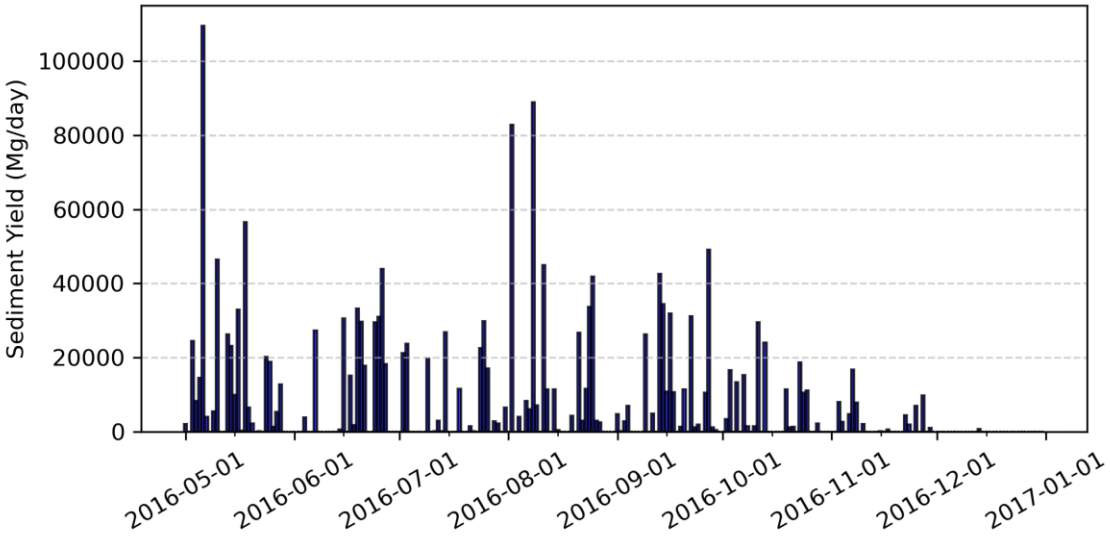

(b)

Extended Data Figure 1: Daily sediment yield in Namatala river catchment. Panels (a) and (b) are as predicted in 2015 and 2016 respectively. The red markers in panel (a) are the sediment yield observed from a bare runoff plot within the catchment: Assuming a homogeneous catchment, this sediment yield was extrapolated to the entire Namatala River catchment. The runoff plot was installed on a typical upland maize cultivation field at the Mbale District production offices. Its dimensions were 0.49 × 5 m, with the length oriented towards the outlet at a gradient of 4.2 %. The surface was kept bare during the observation period from 2015-Sep-26 to 2016-Apr. Runoff from the plot was collected by a bucket placed in a hole dug at the outlet of the runoff plot. Rainfall at the plot site was measured manually.

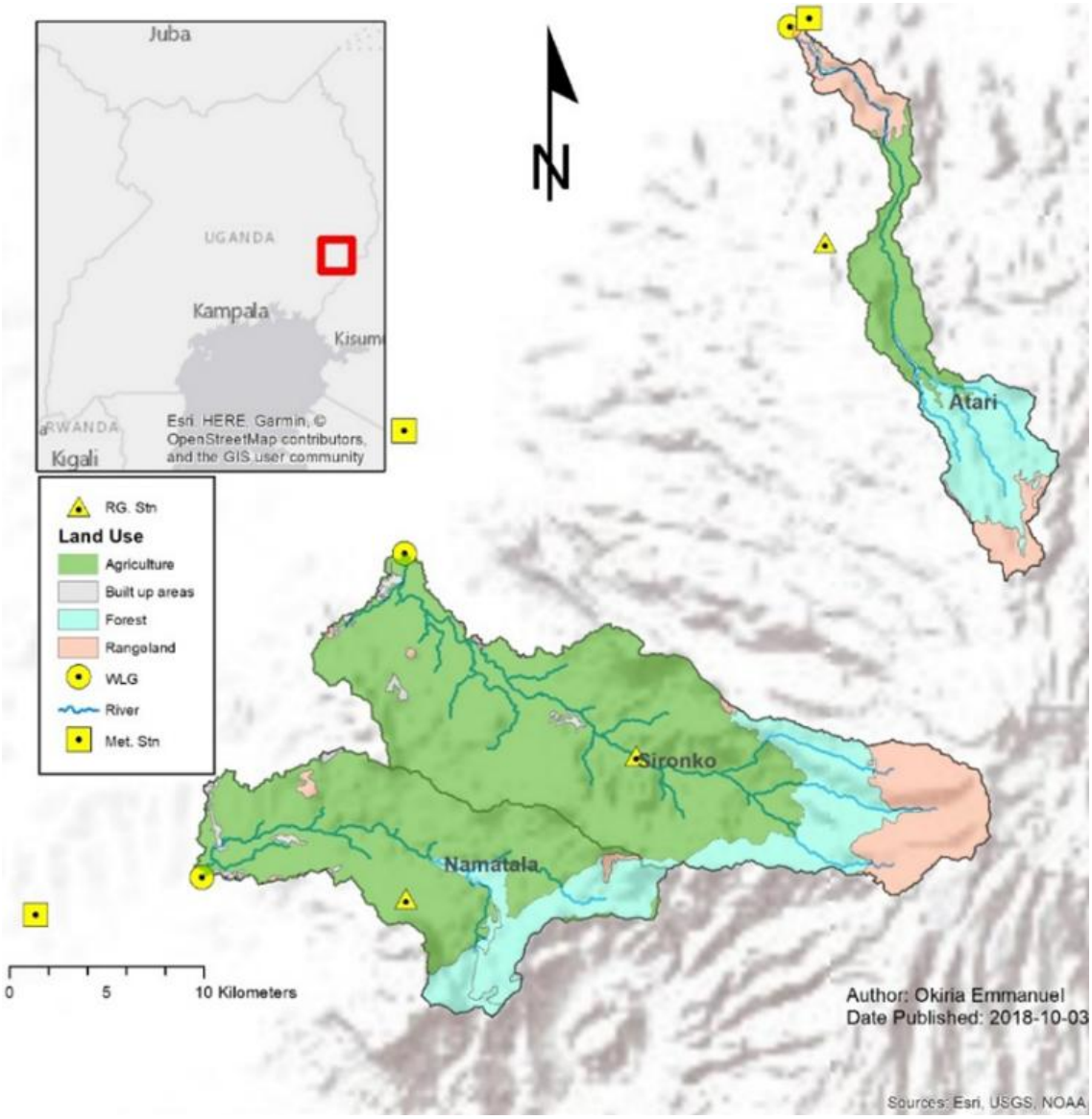

Extended Data Figure 2: Instrumentation and land cover of the Namatala, Atari and Sironko River catchments. Note that RG is rain gauge, WLG is water level gauge and WS is weather station.

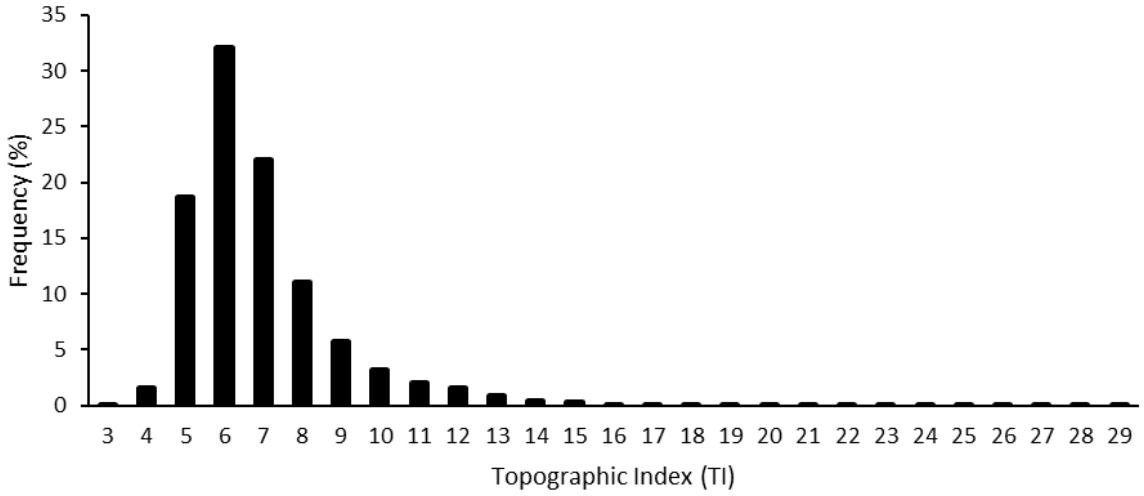

Extended Data Figure 3: Topographic Index distribution of Namatala catchment at 50m grid-resolution.